Brief Communication: Landslides triggered by the $M_s = 7.0$ Lushan earthquake, China

X. L. Chen[1], L. Yu[1], M. M. Wang[2], C. X. Lin[3], C. G. Liu[4], and J. Y. Li[1]

[1]Key Laboratory of Active Tectonics and Volcano, Institute of Geology, China Earthquake Administration,
Beijing, 100029, China
[2]Earthquake Administration of Sichuan Province, Chengdu, 610041, China
[3]Beijing Institute of Geology, Beijing, 100120, China
[4]China Earthquake Networks Center, Beijing, 100045, China

Correspondence to: X. L. Chen (04chxl@sina.com)

Abstract. Earthquake-triggered landslides have drawn much attention around the world because of the severe hazards they pose. The 20 April 2013 $M_s = 7.0$ Lushan Earthquake, which occurred in the Longmen Shan region in Sichuan province, China, triggered more than 1000 landslides throughout an area of about 2200 km^2, and completely blocked many roads and exacerbated overall transportation problems in the mountainous terrain. Preliminary landslide inventory is complied immediately following the earthquake, mainly based on the high-resolution remote sensing images. At the same time, the distribution of these landslides is statistically investigated to determine how the occurrence of landslides correlates with distance from the earthquake epicenter, slope steepness, seismic intensity and rock type. Statistic analysis is conducted using landslide point density (LPD), which is defined as the number of landslides per square kilometer. It is found that LPD has a strong positive correlation with slope gradients and a negative-exponential decline with the distance from the epicenter. The higher LPD values occur in younger strata systems like Quaternary and Tertiary sediments in the study area. Spatially, the triggered landslides are controlled by the causative faults and mainly concentrated around the epicenter. All the landslides are located within the area with seismic intensity $\geq$ VII and in line with seismic intensity. Generally, LPD value decreases with increasing distance from the epicenter, and sometimes landslides are densely distributed along the roads in the mountainous region. Also, this study reveals that the empirical relationship between distance and seismic magnitude is more suitable for estimating the landslide concentration area during the Lushan earthquake compared to other methods.

1 Introduction

At 08:02 LT (Beijing Time) on 20 April 2013, a strong earthquake with $M_s = 7.0$ in surface wave magnitude occurred at the eastern margin of the Tibetan Plateau in Sichuan province, China. Its focal depth was 13 km (http://www.cea.gov.cn/publish/dizhenj/468/553/100342/100343/20130422160312200248983/index.html). The event is named the Lushan earthquake as its epicenter (30.3° N and 103.0° E) was located in the administrative region of Lushan county (Fig. 1). According to a government report, there were 196 people killed in this event (http://www.cea.gov.cn/publish/dizhenj/468/553/100342/100345/20130424151225623554842/index.html).

The $M_s = 7.0$ Lushan earthquake occurred in the southern segment of Longmen Shan range, where a catastrophic earthquake named the Wenchuan earthquake occurred five years earlier (Xu et al., 2008; Yin et al., 2009; Huang et al., 2008; Qi et al., 2010). This recent earthquake occurred to the south of the Wenchuan earthquake, and the distance between these two epicenters is around 90 km.

As it is known that strong earthquakes can trigger many landslides in the mountainous terrain (Keefer, 1984; Bommer et al., 2002; National Institute for Land and Infrastructure Management, Ministry of Land, Infrastructure, Transport

and Tourism, 2004; Yin et al., 2009; Chen et al., 2010), the Lushan earthquake is no exception. Preliminary interpretation of remote sensing images, which are provided by the Institute of Remote Sensing and Digital Earth, Chinese Academy of Sciences and field investigations, which was conducted by the Institute of Geology, China Earthquake Administration, show that more than a thousand of landslides were triggered during this earthquake. However, with respect to the Wenchuan earthquake, the landslides triggered by the Lushan earthquake are smaller both in the amount and the affected area. The phenomenon of two very strong earthquakes occurring successively in the Longmen Shan fault zone (LSFZ) in five years is attractive to scientists, not only for exploring the relation between them, but also for studying the geohazards caused by the Lushan earthquake (Han et al., 2013; Xu et al., 2013).

The occurrence of earthquake-triggered landslides is generally related to the magnitude of ground motion, distance from an earthquake fault or epicenter, rock types, slope gradient and so on (Harp el al., 1981; Keefer, 1984; Wang et al., 2003, 2007; Jibson et al., 2004; Meunier et al., 2007; Qi et al., 2010; Dai et al., 2011; Catani et al., 2013). The Lushan earthquake-triggered landslides provide a good opportunity for statistical analysis of a landslide distribution known to have been produced by an earthquake.

In this study, LPD, defined as the number of landslides per square kilometer and widely used in landslide statistic analysis (Wang et al., 2007; Dai et al., 2011) is used to statistically investigated how the occurrence of landslides correlates with distance from the earthquake epicenter, slope steepness, seismic intensity and rock type. Additionally, it is concluded that the empirical relationship between distance and seismic magnitude is more suitable for estimating the landslide concentrated area for the Lushan earthquake compared to other methods. Also, in order to effectively evaluate the landslide hazard severity, interpretation standards for delimiting landslides should be developed.

2 Tectonic setting

The $M_s = 7.0$ Lushan earthquake occurred at the southern segment of the LSFZ in the eastern margin of the Tibetan Plateau (Han et al., 2013). The LSFZ, which strikes approximately 45° and dips 50–75° toward the northwest (Xu et al., 2008) lies along the middle segment of the Central Longitudinal Seismic Belt (CLSB) of China, and separates the seismically active Tibetan Plateau from the tectonically stable Ordos block, Sichuan basin, and South China block (Zhang et al., 2010). It consists of three sub-parallel thrust faults, namely the Wenchuan–Maowen (F1), Yingxiu–Beichuan (F2) and Guanxian–Anxian (F3) faults, and a frontal blind thrust fault (F4) (Xu et al., 2008; Zhang et al., 2010). During the 2008 Wenchuan earthquake, the event ruptured several strands of this fault zone, and the primary
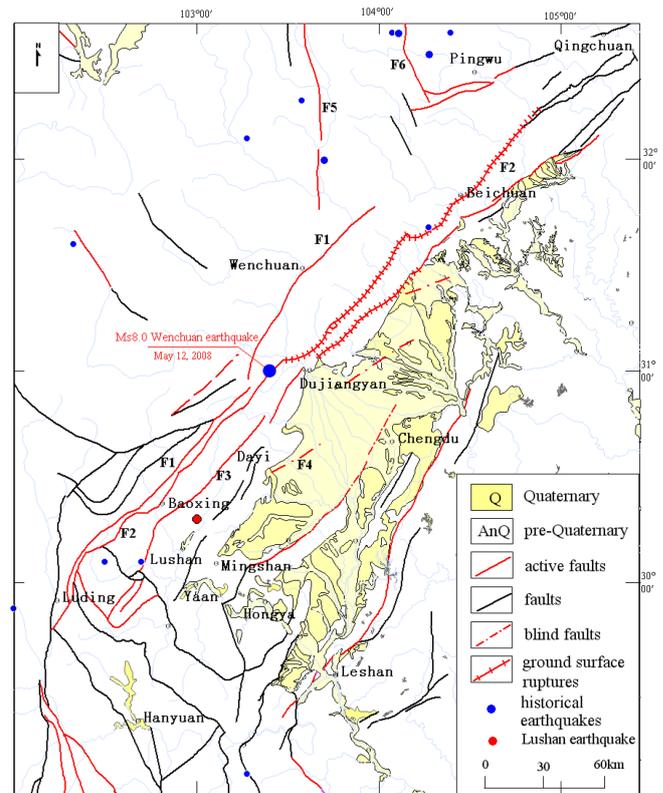
Figure 1. Geological map for the 20 April 2013 $M_s = 7.0$ Lushan Earthquake and the adjacent region (revised from Xu et al., 2009).

rupture is on the Yingxiu–Beichuan strand (Xu et al., 2008; Zhang et al., 2010). Except for these three main faults in the LSFZ, there are others faults and folds developed in this region during the geological evolution (Fig. 1).

The Longmen Shan range is deforming as a result of the collision between the Indian and the Eurasian plates. This has resulted in structural stress accumulation on the collision edges and the release of stress in the fault zone that brought on the catastrophic Wenchuan earthquake, China's most disastrous event since the 1976 Tangshan earthquake (Xu et al., 2008; Zhang et al., 2010). As with the Wenchuan earthquake, the Lushan earthquake was also caused by the slipping of slightly dipping abnormal faults in the deep southern part of Longmen Shan nappe structure zone. The epicenter of the Lushan earthquake was located in the area with increasing Coulomb stress, so that the occurrence of the Wenchuan earthquake may have triggered or accelerated the Lushan earthquake occurrence (Xu et al., 2013).

Unlike the Wenchuan earthquake, which generated long ground surface ruptures, the field investigation after the Lushan earthquake indicated that except for some fracture evidence at the surface, no obvious surface rupture zones were formed (Han et al., 2013). With the understanding of the distribution of relocated aftershocks, focal mechanism solutions and surface structural geology, it is inferred that
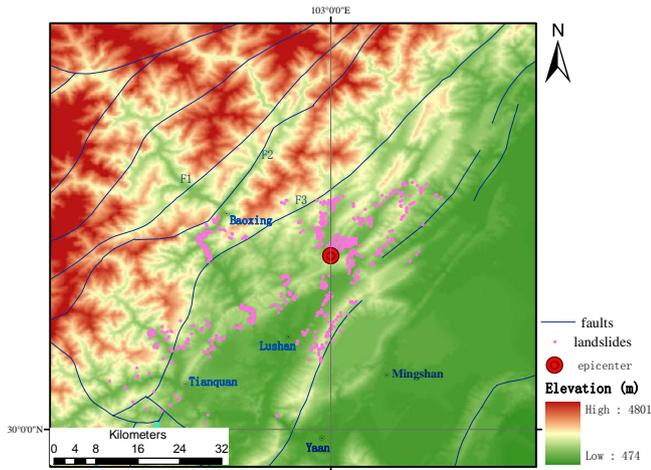
Figure 2. Elevation map for the study region and the landslides triggered by the 20 April 2013 $M_s = 7.0$ Lushan Earthquake (from SRTM, 90 m, http://srtm.csi.cgiar.org/SELECTION/inputCoord.asp).
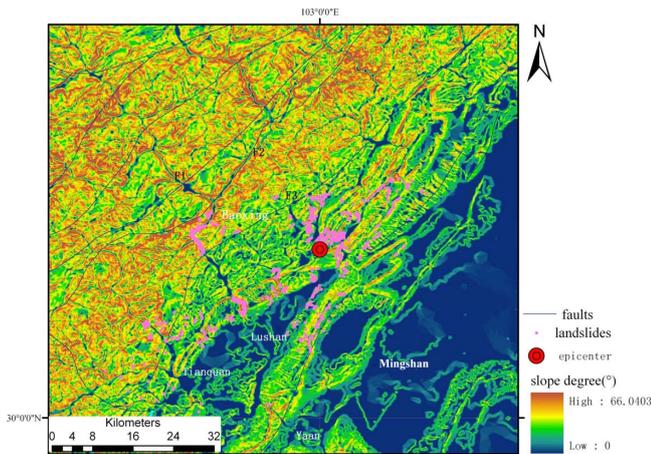
Figure 3. Slope map for the study region and the landslides triggered by the 20 April 2013 $M_s = 7.0$ Lushan Earthquake.

Figure 4. Geological map for the region damaged by the Lushan earthquake (revised from China Geological Survey (CGS), Regional geological map of Sichuan province (1 : 200 000), 2001).

the seismogenic fault of the Lushan earthquake can be classified as a typical blind reverse-fault which strikes 212° and dips toward northwest with a dip angle of 38° ± 2° (Xu et al., 2013).

Topographically, as the transitional zone from the Tibetan Plateau to the Sichuan Basin plain the relief in the Longmen Shan range gradually decreases eastward. To its west, elevations reach more than 4000 m above sea level, while at east of this belt, elevations of the Sichuan Basin lie only 600 m above sea level. On the whole, the elevations in the northwestern region are higher than that in the southeastern, while the reliefs in northwestern side are steeper than in southeastern side. In this study region, the elevations are usually lower than 3000 m (Figs. 2, 3).

The study region has exposures of the strata from the pre-Paleozoic to Quaternary periods. Almost all bedrock appearing in this region are weathered and deformed. Rocks found here mainly include sandstone, mudstone, and shale. Alluvial deposits are developed along the river courses (Fig. 4, Table 1).

The steep western margin of the Sichuan basin is known to be seismically active. The earliest earthquake documented in this region can be traced back to the $M_s = 6.0$ earthquake in September 1327 (Department of Earthquake Disaster Prevention, State Seismological Bureau, 1995). In total, there have been 17 earthquakes with magnitudes ≥ 4.7 in the area subjected to the Lushan earthquake (Xu et al., 2013b). Frequent tectonic activities have created a topography with high mountains intersected by deeply incised valleys and developed a geologically weak region with fragile strata. Therefore, this region is notoriously prone to landslides (Yang et al., 2002; Wang et al., 2008).

3 Landslides generated by the Lushan earthquake

The Lushan earthquake triggered more than 1000 landslides throughout an area of about 2200 km^2, and completely blocked many roads and exacerbated overall transportation problems in the mountainous terrain. As a whole, the landslides triggered by the Lushan earthquake spread in the NE–SW direction, the same as the LSFZ, showing strong influence from the tectonics. Because the southwestern region of the epicenter is occupied by an intermountain basin, land-

Table 1. Simplified strata system of the severely damaged zone by the $M_s = 7.0$ Lushan earthquake (revised after Qi et al., 2010).

Sequence	Symbol	Lithology
Quaternary	Q	Alluvium, Loose deposit
Tertiary	E	Mudstone, sometimes intercalated with mudstone
Cretaceous	K	Conglomerate
Jurassic	J	Sandy slate, mudstone, sandy stone intercalated with mudstone
Triassic	T	Sandy stone, limestone, slate
Permian	P	Thick limestone intercalated slate
Carboniferous	C	Limestone, marble and sandy stone
Devonian	D	Quartzose sandstone
Silurian	S	Sandy stone, phyllite intercalated with limestone
Ordovician	O	Limestone, marble and phyllite of Baota formation
Sinian	Z	Metamorphic sandy stone, metamorphic limestone
Archean	Pt	Granite, diorite, gabbro

slides are absent in the inner basin while continue distributing along the basin sides (Fig. 3). The landslide inventory map as well as the field investigation show that the landslide concentration area is limited to the epicentral region (Figs. 2, 3). Away from the epicenter, landslides were scattered and occurred mainly in the form of rock falls.

3.1 Types of landslides

Landslides are a type of slope movement that can be classified by a combination of material compositions of the sliding mass and the type of movement (Varnes, 1978). During our field investigation, we found that landslides triggered by the Lushan earthquake were of various types. Although sometimes landslides are of more than two failure types, they can be primarily classified into three types, namely rock falls (Fig. 5a), shallow slope failures (Fig. 5b) and rock or soil slides (Fig. 5c), referencing Highland and Bobrowsky (2008).

The area damaged by the Lushan earthquake is covered with fast-growing vegetation (Xu et al., 2013b), so the ground surface failures always have clear scarps and are easily found and delineated during the field investigation, conducted by the Institute of Geology, China Earthquake Administration. Remote sensing images, which are provided by the Institute of Remote Sensing and Digital Earth, Chinese Academy of Sciences were also interpreted. Rock falls are the most common phenomena that can be found on steep slopes along the roads and rivers, with volumes usually less than several tens of cubic meters (Xu et al., 2013b). Shallow slope failures are usually composed of weathered and fractured materials, appearing on gentle-to-moderate slopes where surface slides are likely to occur even without strong shaking. The depth of this kind of landslide is usually less than 1 m and the volumes are in the range from several to several tens cubic meters (Xu et al., 2013b). Rock or soil slides generally have a slide plane which is on surface ruptures or on relatively thin zones of intense shear strain. These kind

of landslides can always produce severe damage because of their large volumes (Highland and Bobrowsky, 2008; Chen et al., 2012b; Xu et al., 2013b).

In this paper, we will only discuss the general distribution features of earthquake-induced landslides and will not distinguish between different types of landslides or discuss the differences.

3.2 Landslide inventory

Landslide inventory is an essential part of seismic landslide hazard analysis (Harp et al., 2011; Guzzetti et al., 2012). Compared with traditional landslide inventory compilation, landslide detection and mapping now benefit from both optical and radar imagery. Many studies and much research on landslides have proved that remote sensing can be considered a powerful instrument for landslide mapping, monitoring and hazard analysis (Qi et al., 2010; Dai et al., 2011; Guzzetti et al., 2012; Tofani et al., 2013; Xu et al., 2013a). For the Lushan earthquake, remote sensing technology plays a vital role in accessing the information in quake disaster areas.

In our study, compilation of landslide inventories is mainly performed by means of interpretation of aerial photography. Because most landslides triggered by the Lushan earthquake had small sizes both in plane area and volume, it is better to map landslides as points which represent the failure sources near the top scarps. Similar to Dai et al. (2011), landslides were identified in the remote sensing images by the following characteristics: (1) landslides scarps showed newly denuded vegetation on the slopes; (2) landslides scarps showed distinct white or brown coloration as compared to the surroundings and (3) landslide debris movement paths could be clearly observed. Individual boulders rock falls are not accounted in this study.

The remote sensing images with resolution of 0.6 m, which are provided by the Institute of Remote Sensing and Digital Earth, Chinese Academy of Sciences, are used in this study. Except for some areas where are covered by clouds

(a) Rock falls

(b) Shallow slope failures

(c) Rock slides

Figure 5. Various landslide types during the 20 April 2013 $M_s = 7.0$ Lushan Earthquake. Photos by M. M. Wang.
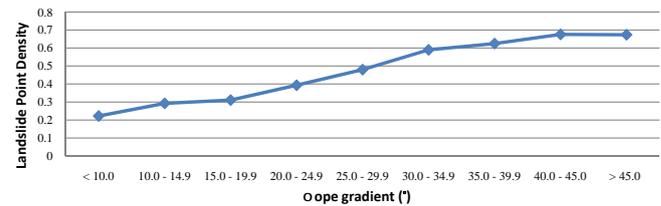
Figure 6. Landslide point density vs. slope gradient in the study area.

and shadows, landslides can be detected easily from the images in the majority of the study region because of the clear scarps they left.

In total, our study show that there are 1129 landslides mapped and the affected area is around 2200 km^2 (Figs. 2, 3). The following analysis on correlating LPD value with distance from the earthquake epicenter, slope gradient, seismic intensity and rock type is based on this affected area.

3.3 Variation of landslide distribution with slope gradient

Much research has shown that topographic features can affect landslide distribution (Qi, 2006; Keefer, 1984, 2006; Dai et al, 2011; Catani et al., 2013). In general, steeper and higher slopes are more prone to landslide activity than gentle slopes (Keefer, 1984; Wang et al., 2007; Dai et al, 2011; Chen et al., 2012b). In this study the Shuttle Radar Topography Mission's digital elevation model (90 m) was used to generate slope angles (Fig. 3), and for each 5° interval of slope gradient, a LPD value was calculated. Because the areas with slope gradient greater than 45° together cover less than 2 % of the total surface area, they are classified in one category. Figure 6 shows the LPD value within each 5° interval of slope gradient. It reveals that LPD values steadily increase with slope gradient.

3.4 Landslide concentration with geological formations

The study area is mainly composed of Mesozoic and Cenozoic strata, which crop out in the eastern side of the region (Fig. 4). Paleozoic and pre-Paleozoic sediments are limited to the northwestern side of the region with higher and steeper relief (Figs. 2, 3, 4).

Our study shows that most of the landslides occurred in the Cretaceous strata, which consist of siltstone, mudstone or mudstone intercalated with shale. These rocks are heavily fractured and always have weak shear strength. So it is reasonable that most of the landslides were concentrated on the slopes consisting of such rocks. Tertiary and Quaternary sediments are present near the epicenter in a comparatively flat plain, therefore, landslides frequently occurred here despite the fact that the relief is generally gentle.

An LPD value is determinate for each geological unit for this study area. Except for Triassic sediments, LPD value
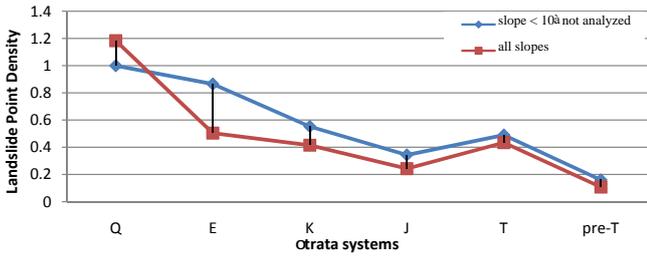
Figure 7. Landslide point density vs. strata systems for the study area.

Figure 8. Landslide distribution with the distance from the epicenter during the 20 April 2013 $M_s = 7.0$ Lushan Earthquake.

decreases with older strata (Fig. 7). The highest LPD value is for the Quaternary system. Though not many landslides (< 30) occurred in the Quaternary sediments, the LPD value is high because of this stratum's smaller area of $20\,km^2$. Without regarding the study area with slopes lower than $10°$ in different strata systems, the larger LPD values appear in the Quaternary and Tertiary sediments. Considering the epicenter location within the geological setting (Figs. 3, 4), it is reasonable that the landslides are prone to concentrated in the near-epicenter area with steeper relief and softer materials.

3.5 Distribution of landslides with the distance to epicenter and seismic intensity

Causative fault is an important factor that can influence the distribution of landslides during a strong shaking event (Khazai and Sitar, 2003; Wen et al., 2004; Wang et al., 2008; Catani et al., 2013). With increasing distance from the causative fault or epicenter, the number of triggered landslides shows a negative-exponential decline (Simonett, 1967; Keefer, 2000; Wang et al., 2007; Chen et al., 2012b).

The $M_s = 7.0$ Lushan earthquake is caused by a blind thrust fault, and there is no obvious surface rupture found during the field investigation which was conducted by the Institute of Geology, China Earthquake Administration soon after the earthquake (http://www.eq-igl.ac.cn/wwwroot/c_000000090002/d_0976.html). Therefore, in this study, the distance to the epicenter is used to analyze the landslide variation. An LPD value is calculated for each 5 km interval centered at the epicenter. The analysis result shows that LPD value decreases with the increasing distance to the epicenter (Fig. 8). More than 90 % of the landslides were located within 30 km of the epicenter.

Based on the Lushan earthquake seismic intensity distribution map issued by China Earthquake Administration (http://www.cea.gov.cn/UploadFile/dizhenj/2013/04/1366973148533.png), it is found that all the landslides are located within the area with seismic intensity $\geq$ VII, and the landslide number is in line with seismic intensity (Fig. 9). In the epicentral region where it has seismic intensity of IX, the LPD value reaches $1.72\,km^2$, which is many times greater than that in the region with seismic intensity of VII (Fig. 10).
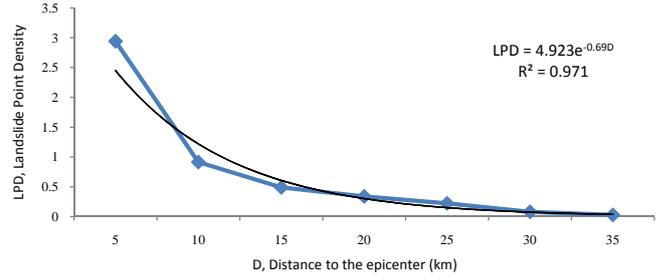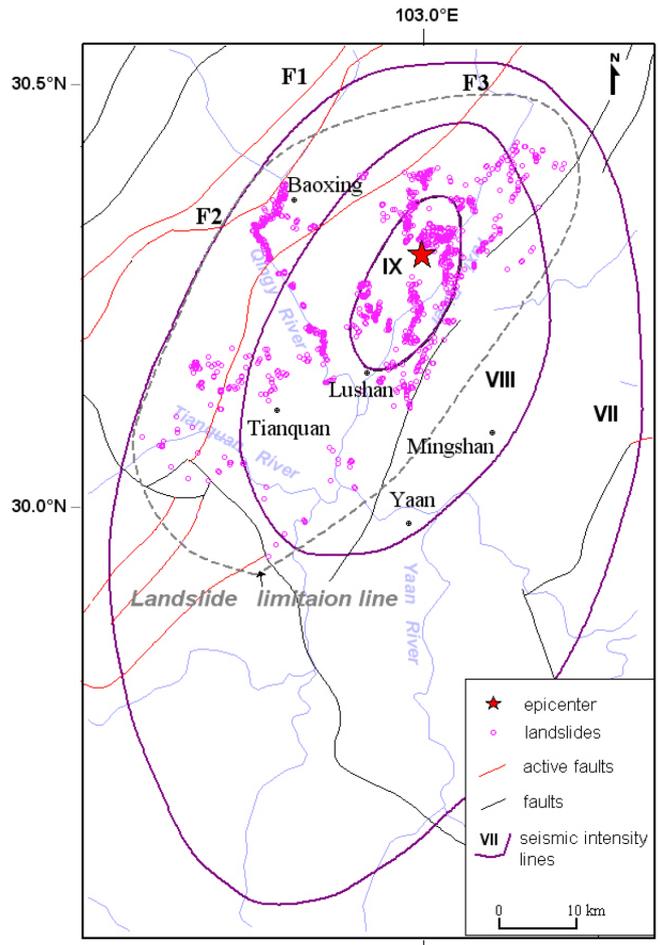
Figure 9. Seismic intensity distribution and the landslide limitation line for the 20 April 2013 $M_s = 7.0$ Lushan Earthquake.

3.6 Distribution of landslides along the roads

Roads or distance to roads have been successfully used in landslide susceptibility assessments because man-made roads can modify the hill slope profile and become an important factor in influencing landslide occurrence (Devkota et al., 2013; Ramakrishnan et al., 2013; Catani et al., 2013). In southwest China, it is a normal phenomenon that landslides
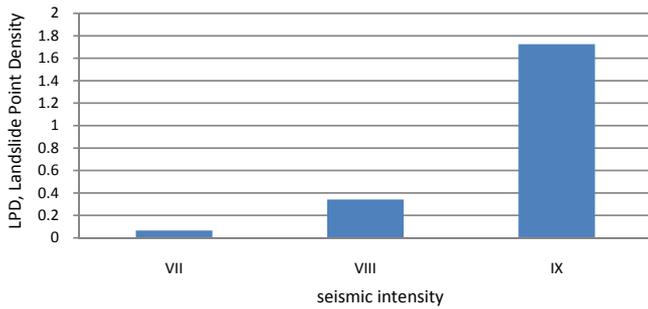
Figure 10. LPD value variation with seismic intensity for the 20 April 2013 $M_s = 7.0$ Lushan Earthquake.

are likely to occur along roads or river banks (Yang et al., 2002; Wang et al., 2008; Chen et al., 2012a), and a strong seismic event will definitely aggravate this kind of geohazard and usually generates landslide dams along river systems (Yin et al., 2009).

In this study region, the relief is typical of high mountains intersected by deeply incised valleys, and roads are usually constructed near rivers. Therefore, after the earthquake, it is found that many landslides were densely developed along roads and river banks, especially in the mountainous areas, which exacerbated overall transportation problems (Fig. 11). For example, there were 79 landslides along 5 km length of Road S210 near Baoxing county (Fig. 11). Our statistics show that more than 20 % of the landslides occurred in a 100 m buffer of the roads during this event.

4 Discussions

4.1 Estimation of the area affected by landslides

The area affected by earthquake-triggered landslides shows strong correlation with earthquake magnitude and earthquakes with larger magnitudes can have larger impact areas (Keefer, 1984; Bommer et al, 2002; Rodríguez et al, 1999). Therefore, seismic magnitude and distance from the epicenter or the causative seismic fault are usually used to judge the limitation boundary of landslide affected area:

1. Kawabe et al. (2000) suggested that the maximum distance (D) from epicenter to landslide can be calculated using

$$\log D = 0.5M - 2.0, \tag{1}$$

   where M is the seismic magnitude, D is the distance in unit of km.

   For the Lushan earthquake, after substituting 7.0 for M in Eq. (1), we obtain $D = 31.6$ km, which is very close to the distance calculated from the landslide inventory in this study, and it is also within the semi-minor axis (33 km) of seismic intensity VII (Fig. 9). Al-

though the maximum distance between a triggered landslide and the epicenter was around 45 km, related analysis shows that more than 90 % of the landslides were located within 30 km from the epicenter.

2. In the study by Keefer, the relationship between the seismic magnitude and the affected area can be expressed as

$$\log_{10} A = M - 3.46(\pm 0.47), \tag{2}$$

   where A is the affected area in unit of square kilometers, M is seismic magnitude for $5.5 < M \leq 9.2$ (Keefer, 2002). Using this equation, the affected area during the Lushan earthquake is calculated to be in the range of 1175–10 232 km^2.

As for the Lushan earthquake, it is located in southwestern China, where landslides triggered by strong earthquakes are mainly located within the area with seismic intensity $\geq$ VII (Earthquake-resistant and damage prevention department of State Seismic Bureau, 1995; Yang et al., 2002; Chen et al., 2012a). Also, for earthquakes with magnitude 7.0 that occurred in southwestern China, the landslide-affected areas range from 2600 to 8843 km^2 (Chen et al., 2012a). According to the Lushan earthquake seismic intensity map issued by the China Earthquake Administration, the area within the seismic intensity line of VII is around 5655 km^2.

In this study, the landslide inventory obtained from interpretation of remote images indicates that the landslides are mainly distributed in the area with seismic intensity $\geq$ VII. They are bounded by the semi-minor axis of intensity VII, but not extended to the southern boundary of the prolate axis of intensity VII (Fig. 9). The affected area is calculated to be 2200 km^2.

Both the empirical relationships between the distance and seismic magnitude (Eq. 1) and seismic magnitude and area (Eq. 2) are used to estimate how widely a given magnitude earthquake can influence a region. However, from this study, it seems that the empirical relationship between the distance and seismic magnitude is a good method to estimate the comparatively concentrated landslide affected area.

4.2 Criteria of landslide size

As mentioned above, both the 2008 $M_s = 8.0$ Wenchuan earthquake and the 2013 $M_s = 7.0$ Lushan earthquake occurred in the LSFZ in succession (Figs. 1, 12). The Wenchuan earthquake occurred to the north of the Lushan earthquake, and the distance between these two epicenters is around 90 km. Unlike the Wenchuan earthquake, which generated 240 km and 90 km long ground surface ruptures (Xu et al., 2008; Yu et al., 2010), the Lushan earthquake did not produce obvious ground surface ruptures (Han et al., 2013).

Landslide distribution during these two earthquakes was extended in the NE–SW direction, the same as the LSFZ
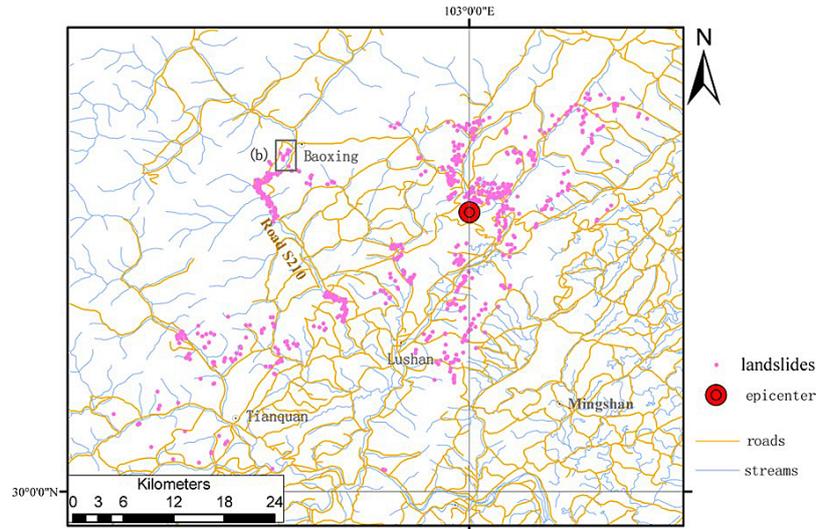
(a) Landslide distribution with the roads and streams
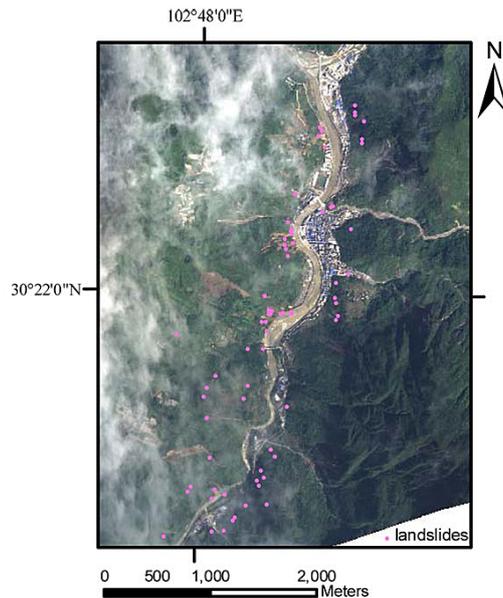
(b) Remote image of the landslides along the road near Baoxing County
(location is indicated in (a); Image provided by the Institute of Remote Sensing and Digital Earth,
Chinese Academy of Sciences)

Figure 11. Landslide distribution with the roads and streams for the 20 April 2013 $M_S = 7.0$ Lushan Earthquake.

striking, indicating the influence of causative faults (Wang et al., 2008; Huang et al., 2008; Chen et al., 2010; Qi et al., 2010; Dai et al., 2011). Although there may be many differences between the landslides triggered by these two earthquakes, the most distinct differences, which can be instantly found from the landslide inventory maps, would be the affected area and the amount of landslides (Fig. 12).

As an essential part of seismic landslide hazard analysis, both the landslide-affected area and landslide quantity are criteria used to evaluate landslide hazard severity (Keefer, 1984; Bommer et al., 2002; Wang et al., 2007). Landslide inventory maps record the location of all landslides that have left discernible features in an area, but sometimes landslide features may not be recognized in the field or through the interpretation of aerial photographs, as they are often obscured by erosion, vegetation, urbanization and anthropic action (Malamud et al., 2004). Although there are many reasons influencing the level of completeness of a landslide
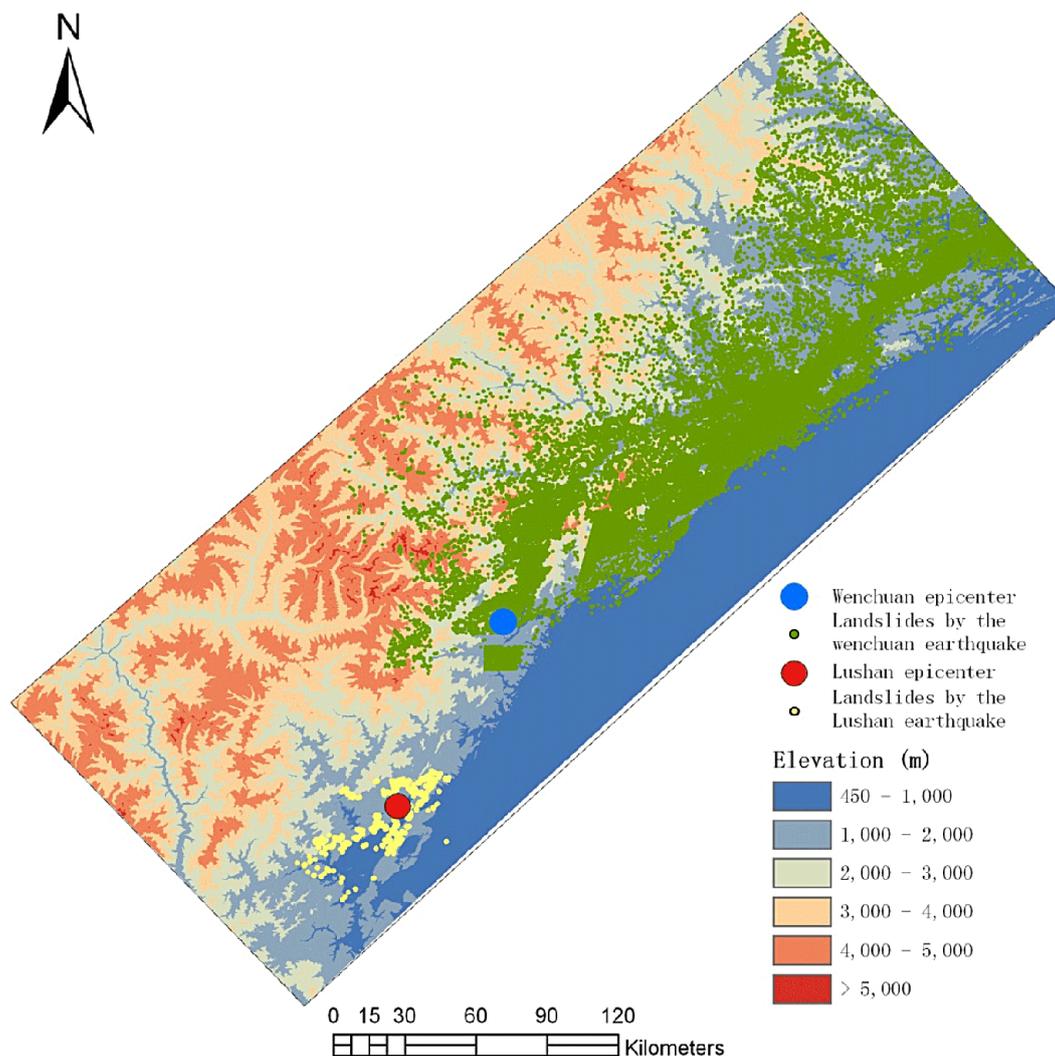
Figure 12. Landslide distribution during the 2008 Wenchuan earthquake (revised from Dai et al., 2011) and the 2013 Lushan earthquake.

inventory, the lack of a uniform definition of landslide size is also an important one. The research of Qi et al. (2012) shows that landslide size has little influence on the distribution characteristics, but sometimes a landslide inventory without uniform size standards can seriously influence the statistics results, especially when calculating LPD values. Exemplified by the Wenchuan earthquake, landslide quantities from different researchers show obvious discrepancies: the quantity ranges from 15 000 (Yin et al., 2009), to 35 000 (Huang et al., 2009) and to 56 000 (Dai et al., 2011). The latest study shows that the number of the landslides triggered by the Wenchuan earthquake is up to 197 481 and distributed over an area of about 110 000 km^2 (Xu et al., 2013a). It is obvious that using the smallest amount of 15 000 individual landslides (Yin et al., 2009) and the largest 197 481 will produce different results. Thus, it is necessary to urgently propose the creation of standards for delimitating landslides in order to improve landslide inventory quality.

5 Conclusions

The $M_s = 7.0$ Lushan earthquake triggered more than 1000 individual landslides throughout an area of 2200 km^2. Although landslide damages from the Lushan earthquake were not as serious as from the Wenchuan earthquake, landslides did completely block many roads and exacerbated overall transportation problems in the mountainous region.

There was no ground surface rupture generated during the Lushan earthquake, nevertheless, landslide spatial distribution still shows domination from the causative faults. Landslides were mainly concentrated around the epicenter and in line with seismic intensity. LPD value decreases with the increasing distance from the epicenter, and more than 90 % of the landslides were located within 30 km distance of the epicenter.

Landslide distribution has a positive correlation with slope gradient. Higher LPD values occur in the young strata

systems composed of soft rocks like mudstone and sandstone. Numerous landslides occurred along the roads and river banks in the mountainous area. Man-made roads in mountainous areas become important factors which must be accounted for when undertaking earthquake-triggered landslide assessments.

Also, it is concluded that the relationship between the distance and seismic magnitude was more precise for estimating the boundary of landslide-affected areas during the Lushan earthquake, and standards for delimitating landslides when doing remote image interpretation should be developed.

References

Bommer, J. J., Carlos, E., and Rodríguez, C. R.: Earthquake-induced landslides in Central America, Eng. Geol., 63, 189–220, 2002.

Chen, X. L., Zhou, B. G., Ran, H. L., Yamamoto, Y., and Hyodo, M.: Geohazards induced by the Wenchuan Earthquake, Geologically Active, Taylor & Francis Group, London, ISBN 978-0-415-60034-7, 2010.

Chen, X. L., Zhou, Q., Ran, H., and Dong, R.: Earthquake-triggered landslides in southwest China, Nat. Hazards Earth Syst. Sci., 12, 351–363, doi:10.5194/nhess-12-351-2012, 2012a.

Chen, X. L., Ran, H. L., and Yang, W. T.: Evaluation of factors controlling large earthquake-induced landslides by the Wenchuan earthquake, Nat. Hazards Earth Syst. Sci., 12, 3645–3657, doi:10.5194/nhess-12-3645-2012, 2012b.

China Geological Survey: Regional geological map of Sichuan Province (1 : 200 000), Geological Press, 2001.

Dai F. C., Xu C., Yao X., Xu L., Tu X. B., and Gong Q. M.: Spatial distribution of landslides triggered by the 2008 $M_\mathrm{s} = 8.0$ Wenchuan earthquake, China, J. Asian Earth Sci., 40, 883–895, 2011.

Densmore, A., Ellis, A., Li, Y., Zhou R. J., Hancock G. S., and Richardson N.: Active tectonics of the Beichuan and Pengguan faults at the eastern margin of the Tibetan Plateau, Tectonics, 26, 1–17, 2007.

Devkota, K. C., Regmi, A. D., Pourghasemi, H. R., Yoshida, K., Pradhan, B., Ryu, I., Dhital, M. R., and Althuwaynee, O.: Landslide susceptibility mapping using certainty factor, index of entropy and logistic regression models in GIS and their comparison at Mugling-Narayanghat road section in Nepal Himalaya, Nat. Hazards, 65, 135–165, 2013.

Department of Earthquake Disaster Prevention?State Seismological Bureau: Catalogue of historical strong earthquakes in China (23rd century B. C. to 1911), Beijing: Seismological Press, 1995 (in Chinese).

Guzzetti, F., Mondini, A. C., Cardinali, M., Fiorucci, F., Santangelo, M., and Chang, K. T.: Landslide inventory maps: new tools for an old problem, Earth Sci. Rev., 112, 42–66, 2012

Haeussler, P. J., Schwartz, D. P., Dawson, T. E., Stenner, H. D., Lienkaemper, J. J., Sherrod, B., Cinti, F. R., Montone, P., Craw, P. A., Crone, A. J., and Personius, S. F.: Surface Rupture and Slip Distribution of the Denali and Totschunda Faults in the 3 November 2002 M 7.9 Earthquake, Bulletin of the Seismological Society of America, 94, 23–52, 2004.

Han, Z. J., Ren, Z. K., Wang, H., and Wang, M. M.: The surface rupture signs of the Lushan "4.20" $M_\mathrm{s} = 7.0$ earthquake at Longmen township, Lushan county and its discussion. Seismology and geology, 35, 388–397. 2013.

Harp, E. L., Keefer, D. K., Sato, H. P., and Yagi, H.: Landslide inventories: the essential part of seismic landslide hazard analyses, Engin. Geol., 122, 9–21, 2011.

Highland, L. M. and Bobrowsky, P.: The landslide handbook – A guide to understanding landslides: Reston, Virginia, US Geological Survey Circular 1325, 129 pp., 2008.

Huang, R. Q. and Li, W. L.: A study on the development and distribution rules of geohazards triggered by "5.12" Wenchuan Earthquake, Chinese J. Rock Mechan. Engin., 27, 2585–2592, 2008 (in Chinese).

Huang , R. Q., Pei, X. J., Zhang, W. F., Li, S. G., and Li, B. L.: Further examination on characteristics and formation mechanism of Daguangbao landslide, J. Engin. Geol., 17, 725–736, 2010 (in Chinese).

Jibson, R. W., Harp, E. L., Schulz, W., and Keefer, D. K.: Landslides triggered by the 2002 M 7.9 Denali Fault, Alaska, earthquake and the inferred nature of the strong shaking, Earthquake Spectra, 20, 669–691, 2004.

Kawabe, H.: Earthquake and earthquake motion, in: Earthquake, edited by: Sabo Nakamura, H., Tsuchiya, S., Inoue, K., and Ishikawa, Y., Kokon Shoin, Tokyo, 1–13, 2000 (in Japanese).

Keefer, D. K.: Landslides caused by earthquakes, Geol. Soc. Amer. Bull., 95, 406–421, 1984.

Keefer, D. K.: Investigating landslides caused by earthquakes – a historical review, Surv. Geophys., 23, 473–510, 2002.

Khazai, B. and Sitar, N.: Evaluation of factors controlling earthquake-induced landslides caused by Chi-Chi earthquake and comparison with the Northridge and Loma Prieta events, Engin. Geol., 71, 79–95, 2003.

Malamud, B. M., Turcotte, D. L., Guzzetti, F., and Reichenbach, P.: Landslide inventory and their statistical properties, Earth Surf. Process. Landforms 29, 687–711, 2004.

Meunier, P., Hovius, N., and Haines, J. A.: Regional patterns of earthquake-triggered landslides and their relation to ground motion, Geophys. Res. Lett., 34, L20408, doi:10.1029/2007GL031337, 2007.

National Institute for Land and Infrastructure Management, Ministry of Land, Infrastructure, Transport and Tourism. A study on methodology for assessing the potential of slope failures during earthquakes, Japan, 2004 (in Japanese).

Qi, S. W., Xu Q., Lan H. X., Zhang B., and Liu J. Y.: Spatial distribution analysis of landslides triggered by 2008.5.12 Wenchuan Earthquake, China, Engin. Geol., 116, 95–108, 2010.

Qi, S. W., Xu, Q., Lan, H. X., Zhang, B., and Liu, J. Y.: Resonance effect existence or not for landslides triggered by 2008 Wenchuan, Engin. Geol., 151, 128–130, 2012.

Ramakrishnan, D., Singh, T. N., Verma, A. K., Gulati, A., and Tiwari, K. C.: Soft computing and GIS for landslide susceptibility assessment in Tawaghat area, Kumaon Himalaya, India, Nat. Hazards, 65, 315–330, 2013.

Rodríguez, C. E., Bommerb, J. J., and Chandlerb, R. J.: Earthquake-induced landslides: 1980–1997, Soil Dynam. Earthquake Engin., 18, 325–346, 1999.

Simonett, D. S.: Landslide distribution and earthquakes in the Bewani and Torricelli Mountains, New Guinea, statistical analysis, in: Landform Studies from Australia and New Guinea, edited by: Jennings, J. N. and Mabbutt, J. A., Cambridge, Cambridge University Press, 64–84, 1967.

Varnes, D. J.: Slope movement types and processes, in: Landslide Analysis and Control, edited by: Schuster, R. L. and Krizek, R. J., National Research Council, Transportation Research Board, Washington, DC, 11–13, 1978.

Wang, H. B., Sassa, K., and Xu, W. Y.: Analysis of a spatial distribution of landslides triggered by the 2004 Chuetsu earthquakes of Niigata Prefecture, Japan, Nat. Hazards, 41, 43–60, 2007.

Wang, W. N., Wu, H. L., Nakamura, H., Wu, S. C., Ouyang, S., and Yu, M. F.: Mass movements caused by recent tectonic activity: The 1999 Chi-chi earthquake in central Taiwan, The Island Arc, 12, 325–334, 2003.

Wang, Y. S., Luo, Y. H., Ji, F., Huo, J. J.,Wu, J. F., and Xu, H. B.:Analysis of the controlling factors on geo-hazards in mountainous epicentre zones of the Wenchuan Earthquake. J. Eng. Geol., 16, 759–763, 2008 (in Chinese).

Wen, B. P., Wang, S. J., Wang, E. Z., and Zhang, J. M.: Characteristics of rapid giant landslides in China, Landslides, 4, 247–261, 2004.

Xu, C., Xu, X. W., Yao, Q., and Wang, Y. Y.: GIS-based bivariate statistical modeling for earthquake-triggered landslides susceptibility mapping related to the 2008 Wenchuan earthquake, China, Quart. J. Engin. Geol. Hydrogeol., 46, 221–236, doi:10.1144/qjegh2012-006, 2013a.

Xu, C., Xu, X. W., Zheng, W. J., Wei, Z. Y., Tan, X. B., Han, Z. J., Li, C. Y., Liang, M. J., Li, Z. Q., Wang, H., Wang, M. M., Ren, J. J., Zhang, S. M., and He, Z. T.: Landslides triggered by the 20 April 2013 Lushan, Sichuan province $M_s = 7.0$ strong earthquake of China. Seismology and geology, 35, 641–660, 2013b.

Xu, Q. and Li, W. L.: Distribution of large scale landslides induced by the Wenchuan earthquake, J. Engin. Geol., 18, 818–826, 2010 (in Chinese).

Xu, X. W., Wen, X. Z., Ye, J. Q., Ma, B. Q., Chen, J., Zhou, R. J., He, H. L., Tian, Q. J., He, Y. L., Wang, Z. C., Sun, Z. M., Feng, X. J., Yu, G. H., Chen, L. C., Chen, G. H., Yu, S. E., Ran, Y. K., Li, X. G., Li, C. X., and An, Y. F.: The $M_s = 8.0$ Wenchuan earthquake surface ruptures and its seismogenic structure, Seismol. Geol., 30, 597–629, 2008.

Xu, X. W. (Eds.): Album of 5.12 Wenchuan 8.0 earthquake surface rupture, China, Seismological Press, 2009.

Xu, X. W., Wen, X. Z., Han, Z. J., Chen, G. H., Li, C. Y., Zheng, W. J., Zhang, S. M., Ren, Z. K., Xu, C., Tan, X. Y., Wang, M. M., Ren, J. J., He, Z., and Liang M. J.: Lushan $M_s7.0$ earthquake: A blind reserve-fault event, Chin. Sci. Bull., 58, 20, doi:10.1007/s11434-013-5999-4, 2013.

Yang, T., Deng, R. G., and Liu, X. L.: The distributing and subarea character of the seismic landslides in Sichuan, J. Mountain Sci., 20, 456–460, 2002 (in Chinese).

Yin, Y. P., Wang, F. W., and Sun, P.: Landslide hazards triggered by the 2008 Wenchuan earthquake, Sichuan, China, Landslides, 6, 139–152, 2009.

Yu, G. H., Xu, X. W., Klinger, Y., Diao, G. L., Chen, G. H., Feng, X. D., Li, C. X., Zhu, A. L., Yuan, R. M., Guo, T. T., Sun, X. Z., Tan, X. B., and An, Y. F.: Fault-Scarp Features and Cascading-Rupture Model for the Mw 7.9 Wenchuan Earthquake, Eastern Tibetan Plateau, China, Bull. Seismol. Soc. Amer., 100, 2590–2614, 2010.

Zhang, P. Z., Wen, X. Z., Shen, Z. K., and Chen, J. H.: Oblique, High-Angle, Listric-Reverse Faulting and Associated Development of Strain: The Wenchuan Earthquake of 12 May 2008, Sichuan, China. Annu. Rev. Earth Planet. Sci., 38, 353–382, 2010.